Secondary Structure of Human Interleukin 2 from 3D Heteronuclear NMR Experiments†

Helen R. Mott,‡ Paul C. Driscoll,‡ Jonathan Boyd,‡ Robert M. Cooke,§ Malcolm P. Weir,§ and Iain D. Campbell*,‡

Department of Biochemistry, University of Oxford, South Parks Road, Oxford OX1 3QU, U.K., and Glaxo Group Research Ltd., Greenford Road, Greenford, Middlesex, UB6 0HE, U.K.

Received April 6, 1992

ABSTRACT: Recombinant ^{15}N-labeled human interleukin 2 (IL-2) has been studied by 2D and 3D NMR using uniformly ^{15}N-labeled protein. Assignment of the backbone resonances has enabled the secondary structure of the protein to be defined. The secondary structure was found to consist of four α-helical regions and a short section of antiparallel β-sheet. This structure is more similar to recent published structures of interleukin 4 and granulocyte–macrophage colony-stimulating factor than to a structure of IL-2 previously obtained from low-resolution X-ray diffraction data.

Interleukin 2 (IL-2) is a 133-residue cytokine secreted by T lymphocytes after stimulation by antigen.[1] IL-2 has a critical role in the progression of T cells from G1 to S phase of the cell cycle. It also stimulates growth of natural killer cells and acts on B cells as a growth factor and stimulus for antibody synthesis (Smith, 1988; Arai et al., 1990). These effects are mediated through a high-affinity receptor (Smith, 1989) which contains at least two subunits of molecular mass 55 and 75 kDa (Saragovi & Malek, 1990). Circular dichroism spectra suggested that IL-2 has a high degree of helical structure with little or no β-sheet (Cohen et al., 1986). This analysis was supported by a low-resolution X-ray diffraction structure (Brandhuber et al., 1987) which showed a bundle of four helices flanked by two shorter helices and poorly defined loops.

As part of a program examining structure–function relationships in growth factors, we have studied the solution conformation of human IL-2 by nuclear magnetic resonance (NMR). In this paper we describe the sequential assignment of the backbone resonances of IL-2 utilizing isotopically labeled protein and heteronuclear three-dimensional (3D) NMR. The secondary structure deduced from this, while being predominantly helical, is quite different from that previously obtained by X-ray diffraction (Brandhuber et al., 1987). The observed secondary structure of IL-2 does, however, bear a strong resemblance to that recently found in two other cytokines, interleukin 4 (IL-4) and granulocyte–macrophage colony-stimulating factor (GM-CSF) (Redfield et al., 1991; Diederichs et al., 1991).

MATERIALS AND METHODS

Human IL-2 was expressed in *Eschericholi coli* as insoluble aggregates and purified by solubilizing in 6 M guanidinium chloride and refolding as described previously (Weir & Sparks, 1987). Uniform ^{15}N labeling of IL-2 was performed by growing the *E. coli* with $[^{15}N](NH_4)_2SO_4$ as the sole nitrogen source. The pure protein (in 44% H_2O/56% CH_3CN containing 0.1% TFA) was dialyzed three times against sodium acetate (10 mM, pH 4.4), then exchanged into sodium acetate-d_3 (10 mM) buffer in 100% D_2O or 90% H_2O/10% D_2O by ultrafiltration, and concentrated to ca. 3 mM.

Heteronuclear NMR spectra was acquired on a home-built spectrometer, interfaced to a GE/Nicolet 1280 computer, operating at 500.1 MHz for ^1H and 50.7 MHz for ^{15}N. Homonuclear experiments were performed on a Bruker AM600 spectrometer. All spectra were acquired at 40 °C, with suppression of the solvent resonance achieved by presaturation or by utilization of a jump–return read pulse (Clore et al., 1983). 3D NOESY-HMQC and HOHAHA-HMQC (Messerle et al., 1989; Driscoll et al., 1990) experiments were acquired as 128 × 32 × 512 complex points using spectral widths of 5102.04, 963.38, and 6024.09 Hz for the $f1$, $f2$, and $f3$ dimensions, respectively. Each 3D spectrum was recorded over a period of about 3 days. A mixing time of 150 ms was employed in the NOESY-HMQC experiment. A WALTZ-16 spin–lock period of 26 ms (Shaka et al., 1983) was used in the HOHAHA-HMQC experiment. 2D HOHAHA and NOESY (Braunschweiler & Ernst, 1983; Jeener et al., 1979; Bax et al., 1987) experiments with spectral widths of 7042.25 Hz in each dimension, were acquired as 1024 × 2048 real points in the $f1$ and $f2$, dimensions respectively. A mixing time of 150 ms was used in the 2D NOESY spectrum. A WALTZ-16 spin–lock period of 40 ms was used in the 2D HOHAHA experiment. Data were processed using the Felix software (Hare Research Inc.) and the Skilling–Brian maximum entropy algorithm (Skilling & Brian, 1984).

RESULTS

The ^1H resonances of IL-2 severely overlapped in 1D and 2D spectra, as expected for a predominantly helical protein of this size. This necessitated the use of ^{15}N labeling and 3D heteronuclear experiments (Driscoll et al., 1990) for the resonance assignments. In the 3D spectra there was also a large degree of resonance overlap, mainly in the $f1$ and $f2$ dimensions. The resolution in these dimensions was, however, improved by using maximum entropy processing (Jones & Hore, 1991a,b).

The heteronuclear 3D spectra were used to correlate $C^\alpha H$ resonances with ^{15}N and ^1H resonances of the backbone amide

† A contribution from the Oxford Centre for Molecular Sciences, which is supported by the U.K. Science and Engineering Research Council and the Medical Research Council. H.R.M. acknowledges the support of Glaxo Group Research. P.C.D. is a Royal Society University Research Fellow.

* To whom correspondence should be addressed.

‡ University of Oxford.

§ Glaxo Group Research.

[1] Abbreviations: IL-2, interleukin 2; IL-4, interleukin 4; GM-CSF, granulocyte–macrophage colony-stimulating factor; NOE, nuclear Overhauser effect; NOESY, nuclear Overhauser effect spectroscopy; HOHAHA, homonuclear Hartmann–Hahn; HMQC, heteronuclear multiple-quantum correlation; TFA, trifluoroacetic acid.

0006-2960/92/0431-7741$03.00/0

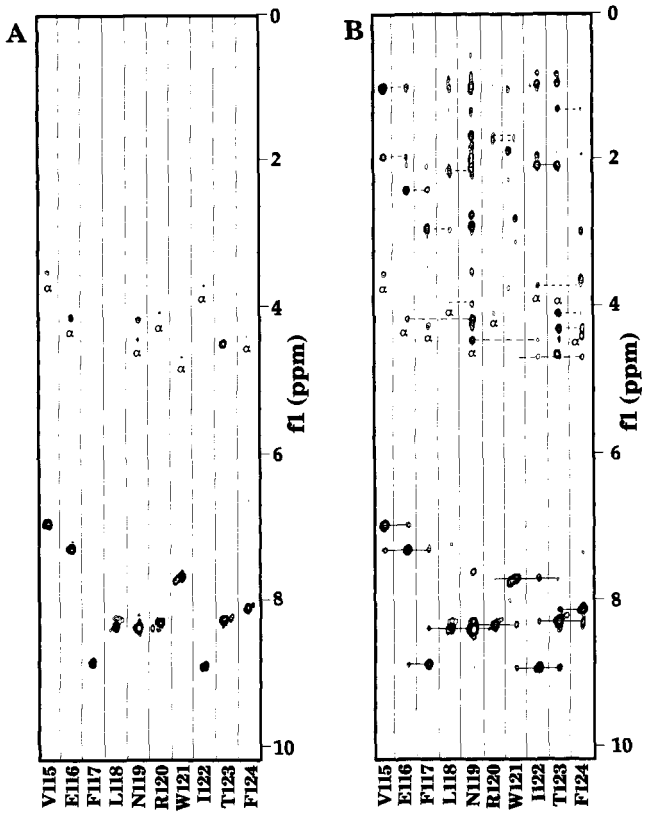

FIGURE 1: Sections from the 3D NMR experiments showing resonances of part of helix D. These plots are made by extracting a strip, 15 points wide, at the ^{15}N chemical shift of the amide NH of interest, from the 3D matrix. (A) HOHAHA-HMQC experiment: the intraresidue NH–C$^{\alpha}$H peaks are marked α. Note that it is not possible to see C$^{\alpha}$H peaks for all residues. In such cases the position of the C$^{\alpha}$H was found from 2D HOHAHA experiments, which usually had better signal to noise ratio. For this part of the amino acid sequence, no correlations beyond C$^{\alpha}$H could be seen. (B) NOESY-HMQC experiment: the NH(i)–NH(i+1), C$^{\alpha}$H(i)–NH(i+1), and a few C$^{\alpha}$H(i)–NH(i+3) NOEs can be observed, although some are obscured by overlap. Intraresidue NH–C$^{\alpha}$H peaks are marked α, NH(i)–NH(i+1) NOEs are marked by solid lines, and C$^{\alpha}$H(i)–NH(i+3) NOEs and side-chain(i)–NH(i+1) NOEs are marked by dashed lines.

groups for individual residues. Where possible these spin system assignments were extended to the side-chain resonances through homonuclear correlations (Wüthrich, 1986). The NOESY-HMQC spectrum identified connectivities between adjacent residues. Most strong sequential NOEs were of the type NH(i)–NH(i+1), but weak C$^{\alpha}$H(i)–NH(i+1) and C$^{\beta}$H(i)–NH(i+1) NOEs were often present, aiding sequential assignment. Thus, stretches of connected residues could be defined by NH(i)–NH(i+1) NOEs, with C$^{\alpha}$H(i)–NH(i+1) and C$^{\beta}$H(i)–NH(i+1) NOEs indicating the directionality. When the segment was long enough to contain several residues with identifiable spin systems, it could be assigned by comparison with the amino acid sequence. An example of the assignment process is shown in Figure 1 for residues Val-115 to Phe-124. By these means, sequential assignments for the backbone resonances of all residues except the five prolines, Lys-76, and Asn-77 could be obtained. The NH resonances of the latter two residues could not be detected, possibly because they are in chemical exchange with the solvent resonance. The neighboring residues in the sequence (Ser-75 and Phe-78) were also found to have weak NH resonances and strong cross peaks at the water frequency in the NOESY-HMQC spectrum, indicating exchange with the bulk solvent.

Figure 2 summarizes the sequential and short-range NOEs observed in spectra of IL-2, which are indicative of the secondary structure of the protein (Wüthrich, 1986). It has also been shown recently that the C$^{\alpha}$H chemical shift values can be used as a convenient indicator of the secondary structure of a protein (Wishart et al., 1992). In this method, the C$^{\alpha}$H chemical shift of all amino acids in the sequence is compared to the corresponding random coil range of chemical shifts. Residues are assigned a chemical shift index of 1, −1, or 0, depending on whether their C$^{\alpha}$H chemical shift is greater than, less than, or equal to the random coil value. Figure 3 shows this chemical shift index for all assigned residues of IL-2.

While the precise positioning of the secondary structure must await detailed structural calculations, the data shown in Figures 2 and 3 indicate that there is a short N-terminal strand, followed by a helix of approximately 19 residues from Gln-11 to Asn-29 (helix A). A loop of around 23 residues leads to helix B, which extends from Leu-53 to Ala-73. The shift data shown in Figure 3 suggest that helix B is less regular than the other three and that the presence of a proline at position 65 causes a downfield shift of the C$^{\alpha}$H resonance of Glu-62. Characteristic helical C$^{\alpha}$H(i)–NH(i+3) NOEs between residues on either side of the proline indicate, however, that the helix is not completely broken by this residue. After helix B there is a short loop of about 7 residues before helix C (Arg-81 to Lys-97). This is followed by another long loop of 18 residues, leading to helix D (Gln-116 to Thr-131). There are some NOEs between backbone resonances indicative of an antiparallel β-sheet pairing residues 44–49 with 107–112, which would account for the downfield shifts of the C$^{\alpha}$H resonances of Tyr-45, Met-46, Pro-47, Tyr-107, Ala-112, Thr-113, and Ile-114. These are the only long-range NOEs that have been assigned so far. Most long-range interactions in helical proteins tend to be between side chains and cannot be detected in ^{15}N heteronuclear experiments. The homonuclear 2D NOESY spectra are too overlapped to interpret the NOEs between side chains.

DISCUSSION

It is clear from the pattern of short- and medium-range NOEs that the secondary structure of IL-2 in solution is dominated by four helices. It is interesting to compare these results with those recently reported for two other cytokines: granulocyte–macrophage colony-stimulating factor (GM-CSF) (Diederichs et al., 1991) and interleukin 4 (IL-4) (Redfield et al., 1991). Both are of a size similar to IL-2 and are comprised of four helices (A–D) with a short, antiparallel β-sheet that links the loop between helices A and B with that between helices C and D. Table I is a comparison of the secondary structures of IL-2, IL-4, and GM-CSF. The similarities in the lengths and positions of the helices and the lengths of the joining loops suggest that the up–up–down–down alignment of helices observed in GM-CSF and IL-4 is maintained in IL-2. GM-CSF and IL-4 each contain a disulfide bond in a position similar to that in IL-2, and the position of the β-sheet is equivalent in all three proteins. Thus, the structural homology is clear, even without significant sequence homology. Figure 4 shows an outline structure of IL-2 predicted from our data and the known structural topology of IL-4 and GM-CSF.

The NMR results described here contradict the previously reported X-ray structure of IL-2. The X-ray structure predicted a core of four helices flanked by two other helices, for which we find no evidence. The sequence positions and lengths of the four main helices also differ in the two structures (Table I). Furthermore, the small β-sheet suggested by the NMR studies, in a position similar to those in IL-4 and GM-CSF, could not be formed in the X-ray structure.

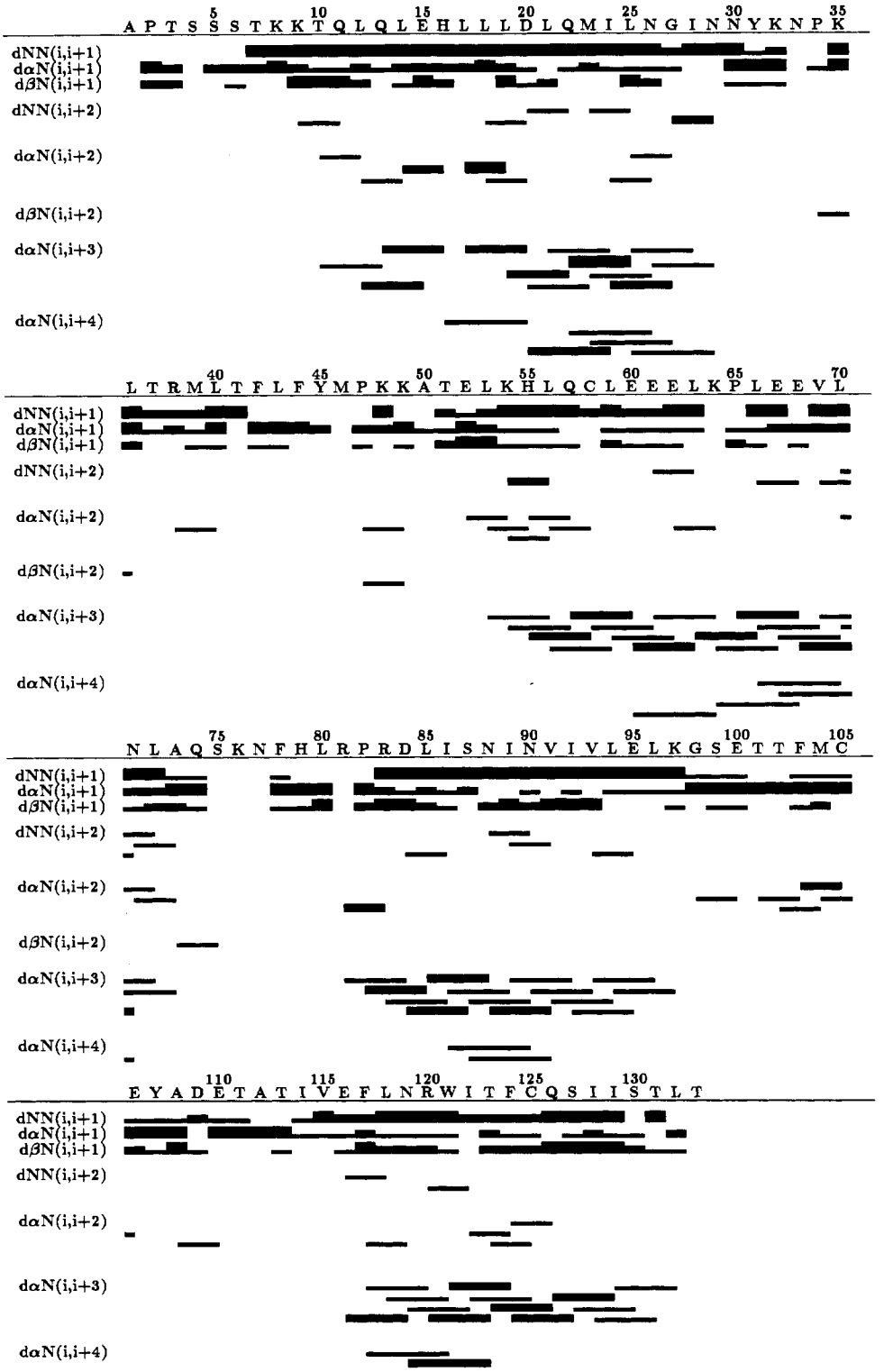

FIGURE 2: Summary of short-range NOEs observed for IL-2. NOEs were classified into strong, medium, or weak, and their approximate strength is indicated by the width of the bar in each case. dNN(i,i+1) refers to a NOE between the backbone NH resonance of residue i and the NH of residue i + 1; dαN(i,i+1) refers to a NOE between the C$^{\alpha}$H resonance of residue i and the backbone NH of residue i + 1. Other NOE types are represented in a similar way (Wüthrich, 1986).

It is interesting to consider the positions of residues which are thought to be important for the biological properties of IL-2 in the light of the proposed IL-2 topology. A combination of mutagenesis studies and computer modeling has led to the hypothesis that residues 8–27 and 33–54 are important in binding to the receptor (Cohen et al., 1986; Weir et al., 1988; Ju et al., 1987; Robb, 1985). The NMR results indicate that these residues are in helix A and the A–B loop. It has also been found that mutation of residues 31–40 in murine IL-2 inactivates the protein and blocks binding to the p70 subunit of the receptor, while mutation of residues 122–128 blocks binding to the p55 subunit but does not affect the activity (Zurawski & Zurawski, 1989). The corresponding residues in human IL-2 are Leu-17 to Asn-26 (helix A) and Tyr-108 to Thr-114 (the C–D loop). Substitution of residue 35, 38, 42, or 43 (in the A–B loop) was found to inhibit binding of human IL-2 to the p55 receptor subunit but did not completely eliminate activity (Sauve et al., 1991). Thus, residues that

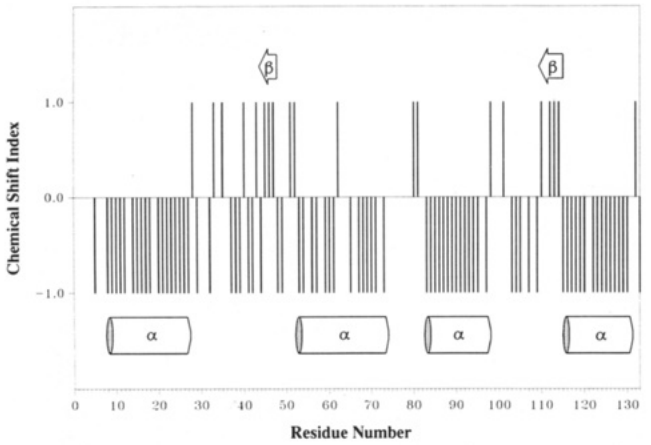

FIGURE 3: Chemical shift index for each residue of IL-2. A grouping of four or more residues with an index of −1 is indicative of an α-helix. A grouping of three or more residues with an index of 1 is indicative of a β-strand. These secondary structure elements are shown as cylinders marked α and arrows marked β, respectively.

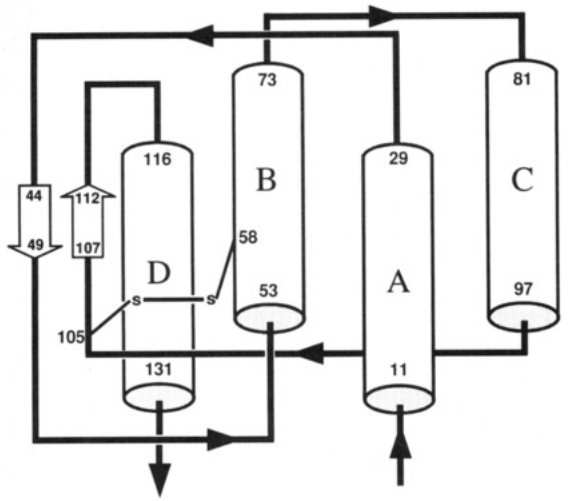

FIGURE 4: Schematic diagram of the structure of IL-2, based on the NMR data and comparison with IL-4 and GM-CSF. The α-helices are shown as cylinders and the β-strands are shown as arrows.

Table I: Comparison of the Secondary Structural Features in GM-CSF, IL-4, and IL-2, Showing Extent of Each Helix, Lengths of Loops between Helices, Positions of β-Sheet Region, and Disulfide Bond which links Helix B to Loop between Helix C and β-Sheet

			IL-2	
	GM-CSF	IL-4	NMR	X-ray[a]
helix A	13–28	5–17	11–29	11–19 33–56
helix B	55–64	41–57	53–73	66–78
helix C	74–87	72–90	81–97	83–101 107–113
helix D	103–116	110–125	116–131	117–133
A–B loop	26	23	23	
B–C loop	9	14	7	
C–D loop	15	19	18	
β-sheet	39–43 98–102	29–31 106–108	44–49 107–112	
disulfides	55–98	46–99	58–105	

[a] The topology of IL-2 in the X-ray structure contains six helices and does not fit with the helix A–D classification given for the other proteins.

are thought to be involved in binding to the p55 chain of the receptor are in the A–B and C–D loops. The data presented here show that the p55-binding residues are in close proximity in the putative 3D structure (Figure 4), since they are adjacent to the β-sheet region. The residues that bind to the p75 chain of the receptor are in helix A, which is on the other side of the molecule. Although a complete understanding of the receptor-binding regions of IL-2 awaits further resonance assignments and calculation of the tertiary structure, it appears that receptor binding is achieved through distinct patches on the surface of IL-2, similar to the situation recently reported for growth hormone (de Vos et al., 1992).

ACKNOWLEDGMENT

We thank B. Bains at Glaxo for his assistance with the production of IL-2. We gratefully acknowledge P. Hodgkin, J. A. Jones, and P. J. Hore for their help with maximum entropy processing.

SUPPLEMENTARY MATERIAL AVAILABLE

Chemical shifts of backbone residues of IL-2 (4 pages). Ordering information is given on any current masthead page.

REFERENCES

Arai, K. F., Lee, A., Miyajima, S., Miyatake, N., & Yokota, T. (1990) *Annu. Rev. Biochem. 59*, 783–836.
Bax, A., Sklenar, V., Clore, G. M., & Gronenborn, A. M. (1987) *J. Am. Chem. Soc. 109*, 7188–7190.
Brandhuber, B. J., Boone, T., Kenney, W. C., & McKay, D. B. (1987) *Science 238*, 1707–1709.
Braunschweiler, L., & Ernst, R. R. (1983) *J. Magn. Reson. 53*, 521–528.
Clore, G. M., Kimber, B. J., & Gronenborn, A. M. (1983) *J. Magn. Reson. 54*, 170–173.
Cohen, F. E., Kosen, P. A., Kuntz, I. D., Epstein, L. B., Ciardelli, T. L., & Smith, K. A. (1986) *Science 234*, 349–352.
Diederichs, K., Boone, T., & Karplus, P. A. (1991) *Science 254*, 1779–1782.
Driscoll, P. C., Clore, G. M., Marion, D., Wingfield, P. T., & Gronenborn, A. M. (1990) *Biochemistry 29*, 3542–3556.
Jeener, J., Meier, B. H., Bachman, P., & Ernst, R. R. (1979) *J. Chem. Phys. 71*, 4546–4553.
Jones, J. A., & Hore, P. J. (1991a) *J. Magn. Reson. 92*, 276–292.
Jones, J. A., & Hore, P. J. (1991b) *J. Magn. Reson. 92*, 363–376.
Ju, G., Collins, L., Kaffka, K. L., Tsien, W.-H., Chizzonite, R., Crowl, R., Bhatt, R., & Kilian, P. L. (1987) *J. Biol. Chem. 262*, 5723–5731.
Messerle, B. A., Wider, G., Otting, G., Weber, C., & Wuthrich, K. (1989) *J. Magn. Reson. 85*, 608–613.
Redfield, C., Smith, L. J., Boyd, J., Lawrence, G. M. P., Edwards, R. G., Smith, R. A. G., & Dobson, C. M. (1991) *Biochemistry 30*, 11029–11035.
Robb, R. J. (1985) *Behring Inst. Mitt. 77*, 56–67.
Saragovi, H., & Malek, T. R. (1990) *Proc. Natl. Acad. Sci. U.S.A. 87*, 11–15.
Sauve, K., Nachman, M., Spence, C., Bailon, P., Campbell, E., Tsien, W.-H., Kondas, J. A., Hakimi, J., & Ju, G. (1991) *Proc. Natl. Acad. Sci. U.S.A. 88*, 4636–4640.
Shaka, A. J., Keeler, J., Frenkiel, T., & Freeman, R. (1983) *J. Magn. Reson. 52*, 335–338.
Skilling, J., & Brian, R. J. (1984) *Mon. Not. R. Astron. Soc. 211*, 111–126.
Smith, K. A. (1988) *Science 240*, 1169–1176.
Smith, K. A. (1989) *Annu. Rev. Cell Biol. 5*, 397–425.
de Vos, A. M., Ultsch, M., & Kossiakoff, A. A. (1992) *Science 255*, 306–312.
Weir, M. P., & Sparks, J. (1987) *Biochem. J. 245*, 85–91.
Weir, M. P., Chaplin, M. A., Wallace, D. M., Dykes, C. W., & Hobden, A. N. (1988) *Biochemistry 27*, 6883–6892.
Wishart, D. S., Sykes, B. D., & Richards, F. M. (1992) *Biochemistry 31*, 1647–1651.
Wüthrich, K. (1986) *NMR of Proteins and Nucleic Acids*, Wiley, New York.
Zurawski, S. M., & Zurawski, G. (1989) *EMBO J. 8*, 2583–2590.